Beam-based Device Positioning in mmWave 5G Systems under Orientation Uncertainties

Elizaveta Rastorgueva-Foi*, Mário Costa†, Mike Koivisto*, Jukka Talvitie*, Kari Leppänen†, and Mikko Valkama*
* Laboratory of Electronics and Communications Engineering, Tampere University of Technology, Finland
† Huawei Technologies Oy (Finland) Co., Ltd, Finland
Email: elizaveta.rastorgueva-foi@tut.fi

***Abstract*—High-accuracy positioning based on angles from multiple base-stations (BSs) requires precise knowledge of the BSs' orientation. Installation errors are bound to occur in practice, and any mismatch between the actual and assumed orientation of the BSs on a given coordinate system leads to systematic errors in the position estimates. In this paper, we consider a system in which BSs transmit reference-signals (RSs) by means of static beams. The directions of such transmissions are known up to an error that is common to all beams for each BS. Different BSs have independent orientation errors. Users determine the reference-signal-received-power (RSRP) of such directional transmissions by employing receive beams. This is termed beam-RSRP (BRSRP) measurements, and they are reported to the network by the users. We propose an algorithm that jointly estimates the 3D positions of users and the orientation errors of the BSs from reported BRSRP measurements. The proposed algorithm is also applicable to the case of a single moving user. The performance of the proposed solution is assessed on a realistic mmW 5G outdoor deployment simulator at 39 GHz and based on ray-tracing propagation modeling. Results show that for a minimum of three BSs in line-of-sight (LoS) to the user, and an orientation uncertainty in azimuth angle of $\phi \leq 3^\circ$, sub-meter positioning accuracy is achieved in 90% of locations. Such orientation uncertainty is estimated with an accuracy of 0.5° in 98% of locations.**

***Index Terms*—5G networks, beamforming, RSRP, positioning, localization, tracking, direction-of-departure, location-awareness, extended Kalman filter, line-of-sight**

I. Introduction

The adoption of the millimeter wave (mmW) frequency bands by the fifth generation (5G) communication standard calls for the use of directional transmission and reception due to the high path-losses at such frequencies. Directional communication in the mmW radio access network (RAN) usually requires line-of-sight (LoS) channel between base stations (BSs) and user equipments (UEs). Receive and transmit beams are typically designed by means of directions of departure (DoDs) and directions of arrival (DoAs) of the signal path, which is a standard task in many sensor array and multichannel signal processing methods [1], [2]. However, the transition to mmW frequencies drives interest in revisiting direction of arrival (DoA)/direction of departure (DoD) estimation methods as well as beamforming techniques, and tailoring them to meet the practical challenges of the upcoming wireless communications system deployment [3]–[5].

In addition to improved resource utilization, directional communication facilitates high-accuracy positioning of UEs. It was shown in [6] that positioning and tracking of UEs can be achieved by exploiting beam reference signal received power (BRSRP) measurements, i.e. reference signal received power (RSRP) measurements for certain BS-UE beam pairs. BRSRPs allow for high-accuracy estimation of the DoDs of reference signals (RSs) using an extended Kalman filter (EKF), which, in turn, can be used for accurate sequential position estimation and tracking of the moving user in the RAN. In practice, the alignment of the BS antennas with respect to (wrt) the known reference direction during installation is imperfect and subject to errors, which can be described as a mismatch between actual BS orientation and the one assumed by the network. Since knowledge of the antenna position and orientation are used as prior information by DoD estimation algorithms, such alignment uncertainties introduce a bias into the angle estimates, which in turn leads to a performance loss in positioning accuracy.

In this paper, we build upon the two-stage EKF-based positioning scheme presented in [6], and propose a novel algorithm that simultaneously tracks multiple UEs as well as estimates the BSs' orientation uncertainties. In particular, the first-stage EKF, running at the BS level, tracks the DoD of downlink (DL) RS to each UE, while the second-stage EKF, operating at the core network level, fuses these DoD estimates from multiple BSs into UEs' positions and BSs' orientation estimates. This approach can be viewed as an extension of the maximum likelihood estimator (MLE) for simultaneous target positioning and sensor array alignment described in [7]. The problem addressed in [7] similarly concerns DoA-based localization of a set of targets using a sensor array with unknown orientation, but focuses on 2D positioning and batch estimation. In contrast, in our paper we propose a sequential estimator for 3D UE positioning and tracking as wellBS orientation uncertainty.

The rest of the paper is organized as follows. Section II provides the necessary background, summarizes previous results, and presents the system model employed in this paper.

This work was supported by the Doctoral Program of the President of Tampere University of Technology, the Tuula and Yrjö Neuvo Foundation, the Nokia Foundation, the Emil Aaltonen Foundation, and the Finnish Funding Agency for Technology and Innovation (Tekes), under the projects "TAKE-5: 5th Evolution Take of Wireless Communication Networks", and "WIVE: Wireless for Verticals".

Our novel EKF algorithm for tracking UEs' positions and BSs' orientations is given in Section III. Section IV describes the considered deployment scenario and provides extensive simulation results using a ray-tracing channel model. Finally, Section V concludes the paper and outlines our future work.

II. Background

A. Beam-RSRP Measurements

Let $\beta_{i,j} \in \mathbb{R}$ denote the RSRP measurement corresponding to the ith UE receive beam and the jth BS transmit beam. $\beta_{i,j}$ is called BRSRP measurement, and it is typically carried out at the UE followed by quantization and reporting to the BS. In particular, BRSRP measurements are defined as follows

$$\beta_{i,j} = \frac{1}{\mathcal{M}_f} \sum_{k=1}^{\mathcal{M}_f} |[\boldsymbol{y}_{i,j}]_k|^2, \tag{1}$$

$$i = 1, \ldots, \mathcal{M}_{\mathrm{UE}},\ j = 1, \ldots, \mathcal{M}_{\mathrm{BS}}, \tag{2}$$

where $\boldsymbol{y}_{i,j} \in \mathbb{C}^{\mathcal{M}_f}$ denotes the multicarrier observation at the UE in an orthogonal frequency-division multiplexing (OFDM) system. The number of subcarriers is denoted by $\mathcal{M}_f$, while $\mathcal{M}_{\mathrm{UE}}$ and $\mathcal{M}_{\mathrm{BS}}$ denote the number of receive and transmit beams at the UE and BS, respectively. The multicarrier observation vector $\boldsymbol{y}_{i,j}$ may be modeled as follows

$$\boldsymbol{y}_{i,j} = \boldsymbol{S}\boldsymbol{h}_{i,j} + \boldsymbol{n}_{i,j}, \tag{3}$$

where $\boldsymbol{S} \in \mathbb{C}^{\mathcal{M}_f \times \mathcal{M}_f}$ denotes a diagonal matrix composed of transmitted symbols in frequency domain and $\boldsymbol{h}_{i,j} \in \mathbb{C}^{\mathcal{M}_f}$ represents the (possibly fast-fading and frequency-selective) radio propagation channel. Moreover, $\boldsymbol{n}_{i,j} \in \mathbb{C}^{\mathcal{M}_f}$ denotes measurement noise. Concretely, the frequency-domain radio channel vector $\boldsymbol{h}_{i,j}$ includes effects due to multipath propagation, transmit beam j and receive beam i, as well as transmitter (Tx)-receiver (Rx) radio frequency (RF)-chains. Also, the measurement noise in (3) is assumed to be complex-circular Gaussian distributed with zero-mean and covariance $\boldsymbol{C}_n = \sigma_{i,j}^2 \boldsymbol{I}$. The measurement noise for different beam-pairs are further assumed to be uncorrelated, i.e., $\mathbb{E}\{\boldsymbol{n}_{i,j}\boldsymbol{n}_{k,l}^{\mathrm{H}}\} = \boldsymbol{0}$, for $i \neq k$ or $j \neq l$. Here, $\mathbb{E}\{\cdot\}$ denotes the mathematical expectation operator. For the sake of simplicity, the measurement noise variance is assumed to be independent of the beam-pair, i.e. $\sigma_{1,1}^2 = \sigma_{1,2}^2 = \ldots = \sigma^2$, where $\sigma^2 \in \mathbb{R}$ is unknown.

In [6], we have shown that the distribution of BRSRP measurements approaches a Gaussian for increasing number of subcarriers $\mathcal{M}_f$ or signal-to-noise ratio (SNR). In particular, we have the following result

$$\beta_{i,j} \sim \mathcal{N}\left(b_{i,j} + \sigma^2, \tilde{\sigma}^2\right), \tag{4}$$

where $\tilde{\sigma}^2$ in an unknown variance and $b_{i,j} \in \mathbb{R}$ is a product between the jth Tx beam-gain in the DoDs of the propagation paths between BS and UE, and the ith Rx beam-gains in the channel's DoAs as well as the channel's path-weights, and power allocated to the RSs. Next, we review an EKF for tracking the DoD of the LoS path between BS and UE [6]. This is needed for angle based positioning where range estimates may be unavailable.

B. EKF for Angle Estimation

Let $\boldsymbol{\beta}[n] \in \mathbb{R}^{\mathcal{M}_{\mathrm{BS}}}$ denote a collection of reported BRSRP measurements for the nth time-instant. Such a measurement vector is given by $\boldsymbol{\beta}[n] = [\beta_{i^*,1}[n], \ldots, \beta_{i^*,\mathcal{M}_{\mathrm{BS}}}[n]]^{\mathrm{T}}$, where $i^* = \arg\max_{i,j} \beta_{i,j}[n]$. Let also $\boldsymbol{s} \in \mathbb{R}^4$ denote the state-vector of the EKF for angle estimation. In particular, such a state-vector is given by $\boldsymbol{s} = [\vartheta, \varphi, \Delta\vartheta, \Delta\varphi]^{\mathrm{T}}$, where $\vartheta \in [0, \pi]$ and $\varphi \in [0, 2\pi)$ denote the co-elevation and azimuth angles of departure (i.e., from BS to UE) while $\Delta\vartheta$ and $\Delta\varphi$ denote the corresponding rate-of-change. The prediction step of the DoD-EKF is given by [6]

$$\boldsymbol{s}^-[n] = \boldsymbol{F}\boldsymbol{s}^+[n-1] \tag{5}$$

$$\boldsymbol{C}^-[n] = \boldsymbol{F}\boldsymbol{C}^+[n-1]\boldsymbol{F}^{\mathrm{T}} + \boldsymbol{Q}, \tag{6}$$

and the update step is [6]

$$\boldsymbol{C}^+[n] = \left(\boldsymbol{C}^-[n]^{-1} + \boldsymbol{\mathcal{I}}(\boldsymbol{s}^-[n])\right)^{-1} \tag{7}$$

$$\Delta\boldsymbol{s}[n] = \boldsymbol{C}^+[n]\,\boldsymbol{q}(\boldsymbol{s}^-[n]) \tag{8}$$

$$\boldsymbol{s}^+[n] = \boldsymbol{s}^-[n] + \Delta\boldsymbol{s}[n]. \tag{9}$$

Details on the state-transition matrix ($\boldsymbol{F} \in \mathbb{R}^{4\times4}$), state covariance matrix ($\boldsymbol{C} \in \mathbb{R}^{4\times4}$) and state-noise covariance matrix ($\boldsymbol{Q} \in \mathbb{R}^{4\times4}$) as well as on the observed Fisher information matrix (FIM) ($\boldsymbol{\mathcal{I}}(\boldsymbol{s}^-[n]) \in \mathbb{R}^{4\times4}$) and gradient of the log-likelihood function of the state given BRSRP measurements ($\boldsymbol{q}(\boldsymbol{s}^-[n]) \in \mathbb{R}^4$) can be found in [6].

In particular, the DoD-EKF outlined above implicitly exploits the directions of the transmit beams in tracking the DoD. Any mismatch between assumed and actual orientation of transmit beams leads to increased errors in the DoD estimates, typically in the form of bias, and overall performance degradation of UE position estimates.

C. Problem Formulation

Let $\boldsymbol{p}_k \in \mathbb{R}^3$ denote the 3-D position of the kth user in Cartesian coordinates. Let also $(\vartheta_k^\ell[n], \varphi_k^\ell[n])$ denote the DoD of the LoS path between the kth UE and ℓth BS at the nth time-instant. The corresponding estimates from the DoD-EKF are denoted by $(\hat{\vartheta}_k^\ell[n], \hat{\varphi}_k^\ell[n])$. For the sake of simplicity, we focus on uncertainties in the orientation of BSs along the xy-plane. A more general approach would be to allow orientation uncertainties in $SO(3)$, but that is left for future work. In particular, orientation uncertainties in the BSs along the xy-plane lead to biased azimuth-angle estimates, only, and these can be modeled as follows

$$\hat{\varphi}_k^\ell[n] = \varphi_k^\ell[n] + \phi_\ell \mod 2\pi$$
$$k = 1, \ldots, K, \quad \ell = 1, \ldots, L, \tag{10}$$

where $\phi_\ell \in [0, 2\pi)$ denotes the orientation uncertainty of the ℓth BSs. Note that such an uncertainty is assumed to be time-invariant.

The problem addressed in this paper can now be formulated as follows; see also Fig. 1. Given DoD estimates between K UEs and L BSs track the locations of such K UEs ($\{\boldsymbol{p}_k\}_{k=1}^K$) as well as the orientation uncertainties of the L BSs ($\{\phi_\ell\}_{\ell=1}^L$).

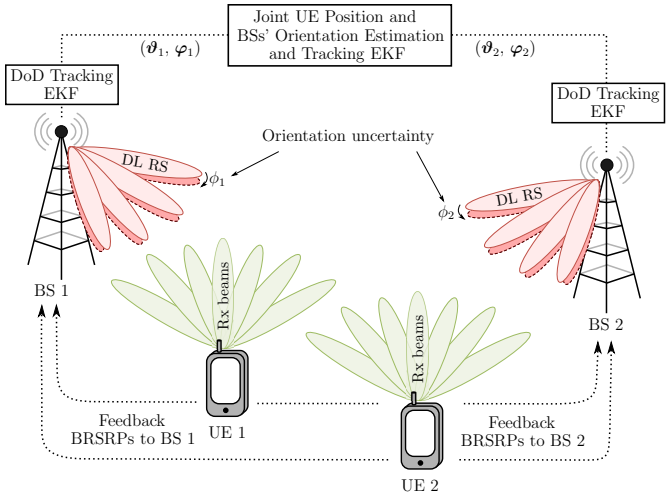

Fig. 1: Illustration of the problem addressed in this paper and proposed architecture. Each BS, possibly having a small orientation misalignment, transmits DL-RSs in a beamformed manner. Based on received DL-RSs, each active UE first measures BRSRPs for each BS and then reports the quantized BRSRPs to the corresponding BSs in a feedback channel. Such BRSRPs measurements are thereafter used in estimating and tracking the DoDs at the BSs in order to finally allow for joint positioning and orientation uncertainty estimation as well as user tracking at a central unit of the network.

III. EKF for Joint User Positioning and BS Orientation Uncertainties

In this section we propose a novel EKF for simultaneous tracking of UEs' 3D positions and orientation uncertainties from all BSs. The proposed algorithm may be understood as an extension of the MLE proposed in [7] to 3D positioning and moving UEs. In particular, the algorithm proposed in [7] is a batch estimator, and thus requires finding the optimum of the (highly nonlinear) log-likelihood function (LLF) every time a UE moves. The EKF proposed in this section is a sequential estimator, and therefore allows for updating the position estimates of all UEs as well as the estimates of BSs' orientation uncertainties whenever new BRSRP measurements are acquired.

Let $\boldsymbol{\vartheta}[n] \in \mathbb{R}^{KL}$ and $\boldsymbol{\varphi}[n] \in \mathbb{R}^{KL}$ denote vectors containing the co-elevation and azimuth angles among the K UEs and L BSs, at the nth time-instant, as follows

$$\begin{aligned}\boldsymbol{\vartheta}[n] &= [\vartheta_1^1[n], \ldots, \vartheta_1^L[n], \vartheta_2^1[n], \ldots, \vartheta_K^L[n]]^{\mathrm{T}},\\ \boldsymbol{\varphi}[n] &= [\varphi_1^1[n], \ldots, \varphi_1^L[n], \varphi_2^1[n], \ldots, \varphi_K^L[n]]^{\mathrm{T}}.\end{aligned} \tag{11}$$

Vectors $\hat{\boldsymbol{\vartheta}}[n] \in \mathbb{R}^{KL}$ and $\hat{\boldsymbol{\varphi}}[n] \in \mathbb{R}^{KL}$ denote the corresponding estimates obtained from the DoD-EKF given in Section II. Such estimates can be assumed to be given by

$$\begin{bmatrix}\hat{\boldsymbol{\vartheta}}[n]\\ \hat{\boldsymbol{\varphi}}[n]\end{bmatrix} \sim \mathcal{N}\left(\begin{bmatrix}\boldsymbol{\vartheta}[n]\\ \tilde{\boldsymbol{\varphi}}[n]\end{bmatrix}, \boldsymbol{C}[n]\right), \tag{12}$$

where $\tilde{\boldsymbol{\varphi}}[n] \in \mathbb{R}^{KL}$ denote the azimuth angles influenced by the BSs' orientation uncertainties; see (10). Moreover, $\boldsymbol{C}[n] \in \mathbb{R}^{2KL \times 2KL}$ is given by

$$\boldsymbol{C}[n] = \mathrm{blkdiag}\left\{\boldsymbol{C}_1^1[n], \ldots, \boldsymbol{C}_1^L[n], \boldsymbol{C}_2^1[n], \ldots, \boldsymbol{C}_K^L[n]\right\}, \tag{13}$$

where $\mathrm{blkdiag}\{\cdot\}$ denotes a block-diagonal matrix and $\boldsymbol{C}_k^\ell[n] \in \mathbb{R}^{2\times 2}$ equals the upper-left (2×2) block of $\boldsymbol{C}^+[n]$ in the DoD-EKF for the kth UE and ℓth BS. For the sake of simplicity $\boldsymbol{C}[n]$ is assumed to be independent of $\hat{\boldsymbol{\vartheta}}[n]$ and $\tilde{\boldsymbol{\varphi}}[n]$.

Let the state vector $\boldsymbol{s} \in \mathbb{R}^{6K+2L}$ be now given by

$$\boldsymbol{s} = [\boldsymbol{p}_1^{\mathrm{T}}, \ldots, \boldsymbol{p}_K^{\mathrm{T}}, \boldsymbol{\phi}^{\mathrm{T}}, \Delta\boldsymbol{p}_1^{\mathrm{T}}, \ldots, \Delta\boldsymbol{p}_K^{\mathrm{T}}, \Delta\boldsymbol{\phi}^{\mathrm{T}}]^{\mathrm{T}}, \tag{14}$$

where $\boldsymbol{\phi} \in \mathbb{R}^L$ denotes the orientation uncertainties of the L BSs. Moreover, vectors $\Delta\boldsymbol{p}_k \in \mathbb{R}^3$ and $\Delta\boldsymbol{\phi} \in \mathbb{R}^L$ denote the corresponding rate-of-change. The prediction step of the EKF is now given by

$$\boldsymbol{s}^-[n] = \boldsymbol{F}\boldsymbol{s}^+[n-1] \tag{15}$$

$$\boldsymbol{C}^-[n] = \boldsymbol{F}\boldsymbol{C}^+[n-1]\boldsymbol{F}^{\mathrm{T}} + \boldsymbol{Q}, \tag{16}$$

where $\boldsymbol{F} \in \mathbb{R}^{(6K+2L)\times(6K+2L)}$, $\boldsymbol{C} \in \mathbb{R}^{(6K+2L)\times(6K+2L)}$, and $\boldsymbol{Q} \in \mathbb{R}^{(6K+2L)\times(6K+2L)}$ denote the state-transition matrix, state covariance matrix, and state-noise covariance matrix, respectively. Similarly to the DoD-EKF, matrices $\boldsymbol{F}$ and $\boldsymbol{Q}$ can be found from [8, Ch.2] by noting that we have employed a continuous white-noise acceleration model for both UEs' and orientation uncertainties' state-dynamics. The update step of the EKF is

$$\boldsymbol{C}^+[n] = \left(\boldsymbol{C}^-[n]^{-1} + \boldsymbol{\mathcal{I}}(\boldsymbol{s}^-[n])\right)^{-1} \tag{17}$$

$$\Delta\boldsymbol{s}[n] = \boldsymbol{C}^+[n]\,\boldsymbol{q}(\boldsymbol{s}^-[n]) \tag{18}$$

$$\boldsymbol{s}^+[n] = \boldsymbol{s}^-[n] + \Delta\boldsymbol{s}[n], \tag{19}$$

where $\boldsymbol{\mathcal{I}}(\boldsymbol{s}^-[n]) \in \mathbb{R}^{(6K+2L)\times(6K+2L)}$ and $\boldsymbol{q}(\boldsymbol{s}^-[n]) \in \mathbb{R}^{(6K+2L)}$ denote the observed FIM and gradient of the log-likelihood function of both UEs' positions and BSs' orientation uncertainties given DoD estimates from multiple BSs.

In particular, let $\boldsymbol{m} \in \mathbb{R}^{2KL}$ denote the estimated DoDs of L BSs towards K UEs, i.e. $\boldsymbol{m} = [\hat{\boldsymbol{\vartheta}}^{\mathrm{T}}, \hat{\boldsymbol{\varphi}}^{\mathrm{T}}]^{\mathrm{T}}$, and $\boldsymbol{\xi} = [\boldsymbol{p}_1^{\mathrm{T}}, \ldots, \boldsymbol{p}_K^{\mathrm{T}}, \boldsymbol{\phi}^{\mathrm{T}}]^{\mathrm{T}}$. It follows from (12) that $\boldsymbol{m} \sim \mathcal{N}(\boldsymbol{\mu}(\boldsymbol{\xi}), \boldsymbol{C})$, where

$$\boldsymbol{\mu}(\boldsymbol{\xi}) = \left[\boldsymbol{\vartheta}^{\mathrm{T}}(\boldsymbol{\xi}), \tilde{\boldsymbol{\varphi}}^{\mathrm{T}}(\boldsymbol{\xi})\right]^{\mathrm{T}} \tag{20}$$

$$\boldsymbol{C} = \mathrm{blkdiag}\left\{\boldsymbol{C}_1^1, \ldots, \boldsymbol{C}_1^L, \boldsymbol{C}_2^1, \ldots, \boldsymbol{C}_K^L\right\}. \tag{21}$$

Note that

$$\vartheta_k^\ell(\boldsymbol{\xi}) = \arctan\left(\frac{-\Delta z_k^\ell}{d_{2D_k^\ell}}\right) + \pi/2 \tag{22}$$

$$\tilde{\varphi}_k^\ell(\boldsymbol{\xi}) = \arctan 2\left(\Delta y_k^\ell, \Delta x_k^\ell\right) + \phi_\ell, \tag{23}$$

where $d_{2D_k^\ell} = \sqrt{\Delta {x_k^\ell}^2 + \Delta {y_k^\ell}^2}$, $\Delta x_k^\ell = x_{\mathrm{UE}_k} - x_{\mathrm{BS}_\ell}$, $\Delta y_k^\ell = y_{\mathrm{UE}_k} - y_{\mathrm{BS}_\ell}$, and $\Delta z_k^\ell = z_{\mathrm{UE}_k} - z_{\mathrm{BS}_\ell}$. The gradient of the log-likelihood function of $\boldsymbol{\xi}$ given $\boldsymbol{m}$, and respective observed FIM, now follow from [9, Ch.3]

$$[\boldsymbol{q}(\boldsymbol{\xi})]_m = \left(\frac{\partial\boldsymbol{\mu}(\boldsymbol{\xi})}{\partial[\boldsymbol{\xi}]_m}\right)^{\mathrm{T}} \boldsymbol{C}^{-1}\left(\boldsymbol{m} - \boldsymbol{\mu}(\boldsymbol{\xi})\right) \tag{24}$$

$$[\boldsymbol{\mathcal{I}}(\boldsymbol{\xi})]_{m,n} \approx \left(\frac{\partial\boldsymbol{\mu}(\boldsymbol{\xi})}{\partial[\boldsymbol{\xi}]_m}\right)^{\mathrm{T}} \boldsymbol{C}^{-1}\frac{\partial\boldsymbol{\mu}(\boldsymbol{\xi})}{\partial[\boldsymbol{\xi}]_n}. \tag{25}$$

Note that $\boldsymbol{q}(\Delta\boldsymbol{\xi}) = \boldsymbol{0}$, and similarly for $\boldsymbol{\mathcal{I}}(\Delta\boldsymbol{\xi})$, where $\Delta\boldsymbol{\xi} = [\Delta\boldsymbol{p}_1^{\mathrm{T}}, \ldots, \Delta\boldsymbol{p}_K^{\mathrm{T}}, \Delta\boldsymbol{\phi}^{\mathrm{T}}]^{\mathrm{T}}$.

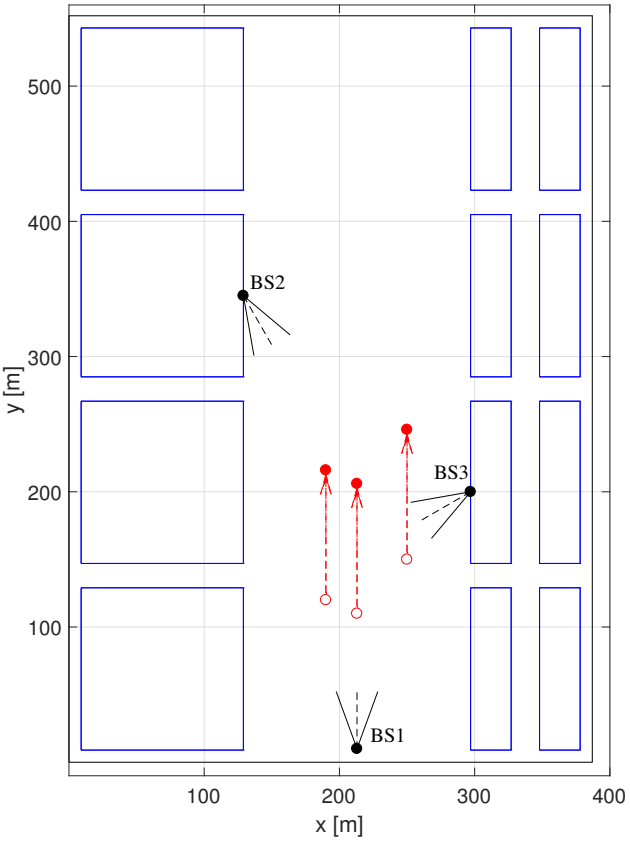

Fig. 2: Illustration of the deployment scenario considered in this paper. The modified Madrid grid is drawn in blue, with a large open area of size 550 m by 150 m. The multipath radio channel between UE and BSs is calculated using the METIS ray-tracing channel model [10].

IV. Numerical Results

A. Deployment Scenario and System Parameters

Our numerical study considers the so-called Madrid grid, widely used in Mobile and Wireless Communications Enablers for the Twenty-Twenty Information Society (METIS) project [10]. METIS Madrid grid is well documented, and yields a reproducible radio channel model between UE and BSs. For our numerical simulations, such a grid has been modified in order to have an open area with a size of approximately 550 m by 150 m. Three BSs are located near the edges of the open area. The considered layout is illustrated in Fig. 2. The three users move parallel to each other northwards with a constant speed of $2\,\mathrm{m\,s^{-1}}$. The height of all BSs is 50 m, and each BS is equipped with an antenna array featuring 64 fixed 3°-wide beams that span 40° in both co-elevation and azimuth. The maximum gain of the BS beams is ≈30 dBi. Each of BS's beam pattern is oriented in order to cover the area occupied by the UEs: BS1 is oriented along the azimuth angle of $\varphi_1 = 90°$, BS2 along the azimuth of $\varphi_2 = -60°$, and BS3 along the azimuth of $\varphi_3 = -150°$.

Moreover, the height of the UEs is considered to be 1.5 m, and each UE is equipped with a quasi-omnidirectional antenna array with 52 beams spanning 360° in azimuth at a fixed co-elevation of ≈ 75°. The UE beams have 3 dB beamwidth of ≈6° in azimuth and ≈40° in co-elevation, and a maximum gain of ≈17 dBi. In this study, we consider a mmW cellular system operating at 39 GHz with a bandwidth of 100 MHz and a subcarrier spacing of 120 kHz, yielding in total 800 subcarriers. The beam-specific DL-RS transmission is scheduled using orthogonal radio resources. For each of the 64 BS beams, DL-RSs are transmitted with a Tx power of 10 dB. Thereafter, each moving UE measures the DL-RS BRSRP for all 64×52 beam-pairs for all available BSs every 160 ms. The measured BRSRPs, quantized using 7 bits in the range of $[-140, -44]$ dBm, are then communicated back to the corresponding BS, thus following the RSRP reporting scheme proposed in 5G Rel. 15 [11].

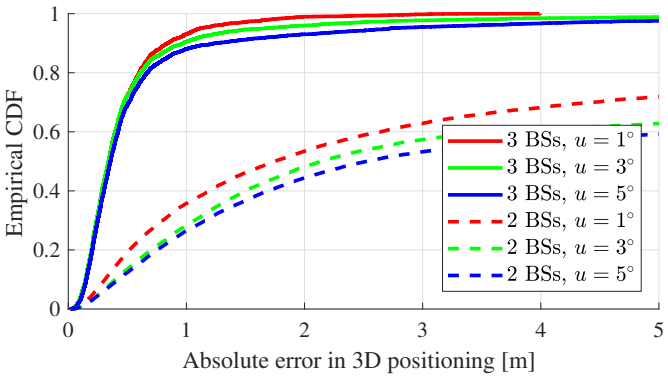

Fig. 3: Empirical cumulative distribution function (CDF) of the 3D position error for three UEs. Deployment scenario employing all three BSs (solid lines) is compared to the combinations of two BSs (dashed lines). Colour codes different values of introduced orientation uncertainty: red corresponds to $u = 1°$, green to $u = 3°$, and blue to $u = 5°$

B. Performance of the Proposed Positioning Scheme

The performance of the positioning algorithm proposed in Section III is assessed with a group of three UEs moving along parallel routes with a constant speed of $2\,\mathrm{m\,s^{-1}}$ as depicted in Fig. 2. The UEs start and stop simultaneously, and the DL-RSs are scheduled at the same time. Furthermore, the orientation uncertainty is simulated by means of introducing angle uncertaities ϕ_i to the assumed azimuth angles φ_i, where $i \in \{1, 2, 3\}$ is a BS index. which describe the orientation of the BS antenna array patterns in the horizontal plane in the global reference frame. In order to study the impact of the orientation uncertainty on the performance, we chose three different scenarios with $\phi_i \sim \mathcal{U}([-u, u])$, where $\mathcal{U}$ denotes a uniform distribution and $u \in \{1°, 3°, 5°\}$. In particular, the addition of ϕ_i can be also understood as a rotation of the whole beam pattern of the i-th BS by the amount of ϕ_i (see Fig. 1). The directions of these beam rotations for different BSs are considered independent, thus in the numerical study, the rotation directions were chosen so that the simulation always includes BSs with both clockwise and counter-clockwise rotation.

In this paper, the key performance indicators of the positioning scheme are 3D position and BS orientation estimation accuracy. The obtained empirical CDFs of the absolute errors in 3D position and BS orientation are given in Figs. 3 and 4, respectively. The plots demonstrate results obtained via two

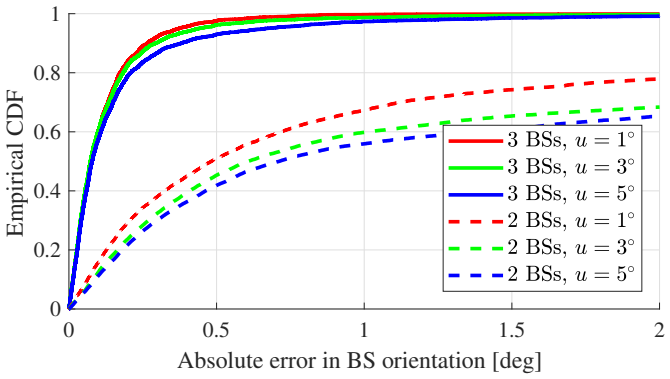

Fig. 4: Empirical CDF of the orientation uncertainty estimation error for three UEs.Deployment scenario employing all three BSs (solid lines) is compared to the cases of all possible combinations of two BSs (dashed lines). Colour codes different values of introduced orientation uncertainty: red is $u = 1°$, green is $u = 3°$, and blue is $u = 5°$

groups of simulations: first group includes all three available BSs, and the second group includes different pairs of BSs. In each group, simulations were performed for all three values of the limiting BS orientation uncertainty, i.e., $u \in \{1°, 3°, 5°\}$.

As demonstrated by Figs. 3 and 4, UEs' positioning accuracy is influenced by the orientation uncertainty u. In particular, for the group of simulations using three BSs, an accuracy of $1\,\mathrm{m}$ is achieved in 93% of locations for $u = 1°$, in 90% of locations for $u = 3°$ and in 88% of the locations for $u = 5°$. For the simulations with two BSs, the positioning accuracy is substantially lower than that required by 5G positioning applications. Also, the discrepancy between the positioning accuracy and BS orientation accuracy for this group of simulations is larger than that with three BSs, which is due to the fact that larger orientation uncertainties cause slower EKF convergence, whereas simulations with three BSs do not demonstrate this effect. Thus, sub-meter accuracy in 90% of locations with our positioning scheme is achievable for the simulation involving three UEs and three BSs for an orientation uncertainty in azimuth angle of $\phi \leq 3°$. Orientation uncertainty is estimated with an accuracy of $0.5°$ in 98% of locations for this group of simulations. Also, for two-BSs simulations, accuracy of BS orientation uncertainty estimation became substantially lower.

V. Conclusion

In this paper we present a DoD-based user positioning technique for mmW communications systems under BS orientation uncertainties in azimuth angle employing transmit and receive beamforming. Such a mismatch between the assumed and actual orientation of the BS can occur as a result of installation errors. The first stage of the two-stage positioning scheme consists of sequential EKF estimation of the DL RS DoDs, based on the BRSRP measurements that UE reports to the BS. The second stage EKF filter uses these DoD estimates to track the positions of the UEs and orientation uncertainties of the BSs. We assess the performance of the proposed solution with realistic mmW 5G outdoor deployment numerical simulations at 39 GHz, based on ray-tracing propagation modeling. Results show that sub-meter positioning accuracy is achieved in 88% of locations for orientation uncertainties of up to $5°$, and 90% of locations for orientation uncertainties of up to $3°$. The accuracy of orientation uncertainty estimation is $0.5°$ in 98% of locations. In the considered setup, such accuracy of the UE position and BS orientation estimates is obtained with a minimum number of three BSs in LoS condition. For the evaluation setup with two active BSs in LoS, accuracies of the 3D positioning and BS orientation uncertainties are substantially lower and do not meet the 3GPP requirements. Also, in this case the value of orientation uncertainty, u, impacts the convergence time of the EKFs.

In future work, we plan to consider estimation of 3D orientation uncertainties of BSs. Moreover, a larger amount of UEs and numerical simulations for a variety of the trajectories need to be included to make the numerical simulations more realistic. These extensions of the simulator would allow us to study UE positioning and tracking in 3D space, including the use cases of unmanned aerial vehicles (UAV).

References

[1] H. Krim and M. Viberg, "Two decades of array signal processing research: the parametric approach," *IEEE Signal Proc. Magazine*, vol. 13, no. 4, pp. 67–94, Jul 1996.

[2] J. Li, B. Sadler, and M. Viberg, "Sensor array and multichannel signal processing," *IEEE Signal Proc. Magazine*, vol. 28, no. 5, pp. 157–158, Sept 2011.

[3] S. Sun, T. Rappaport, R. Heath, A. Nix, and S. Rangan, "MIMO for millimeter-wave wireless communications: beamforming, spatial multiplexing, or both?" *IEEE Comm. Magazine*, vol. 52, no. 12, pp. 110–121, December 2014.

[4] S. Kutty and D. Sen, "Beamforming for millimeter wave communications: An inclusive survey," *IEEE Communications Surveys Tutorials*, vol. 18, no. 2, pp. 949–973, Secondquarter 2016.

[5] T. Rappaport, Y. Xing, G. MacCartney, A. Molisch, E. Mellios, and J. Zhang, "Overview of millimeter wave communications for fifth-generation (5G) wireless networks - with a focus on propagation models," *IEEE Trans. Antennas and Propagation*, vol. 65, no. 12, pp. 6213–6230, Dec 2017.

[6] E. Rastorgueva-Foi, M. Costa, M. Koivisto, K. Leppänen, and M. Valkama, "User Positioning in mmW 5G Networks Using Beam-RSRP Measurements and Kalman Filtering," *21st International Conference on Information Fusion (FUSION)*, pp. 1–7, Jul. 2018.

[7] O. Jean and A. Weiss, "Geolocation by direction of arrival using arrays with unknown orientation," *IEEE Transactions on Signal Processing*, vol. 62, no. 12, pp. 3135–3142, Jun 2014.

[8] J. Hartikainen, A. Solin, and S. Särkkä, "Optimal filtering with Kalman filters and smoothers," 2011. [Online]. Available: http://becs.aalto.fi/en/research/bayes/ekfukf/documentation.pdf

[9] S. Kay, *Fundamentals of Statistical Signal Processing: Estimation Theory*. Prentice-Hall Signal Processing Series, 1993.

[10] METIS, "D1.4 Channel models," Feb. 2015. [Online]. Available: https://www.metis2020.com/wp-content/uploads/METIS_D1.4_v3.pdf

[11] 3GPP, TS38.214, "Physical layer procedures for data," 2018. [Online]. Available: https://portal.3gpp.org/desktopmodules/Specifications/SpecificationDetails.aspx?specificationId=3216